RSC Advances

PAPER

View Article Online
View Journal | View Issue

Cite this: *RSC Adv.*, 2017, **7**, 23011

Equilibrium and kinetic studies on the adsorption of thiophene and benzothiophene onto NiCeY zeolites

Liu Fei,† Jingwei Rui,† Rijie Wang, Yanfei Lu and Xiaoxia Yang *

Received 11th January 2017
Accepted 19th April 2017

DOI: 10.1039/c7ra00415j

rsc.li/rsc-advances

NiCeY zeolites were prepared by ion-exchanging NaY with 0.1 M $Ni(NO_3)_2$ and 0.1 M $Ce(NO_3)_3$ solution. The experiment for the adsorption of thiophene and benzothiophene from a model fuel has been carried out by using the prepared NiCeY. The adsorption isotherms and kinetics of thiophene and benzothiophene in *n*-octane have been studied, and the parameters (ΔH, ΔG, ΔS) for the adsorption were calculated. The effect of adsorption temperature and contact time on the adsorption were investigated through the static method at ambient pressure. The experimental data was analyzed using the pseudo first order and pseudo second order kinetic equations and Langmuir and Freundlich models. The results show that the isotherm equilibrium for thiophene and benzothiophene adsorption can be represented by the Langmuir equation.

1. Introduction

Nowadays, desulfurization of fuels has attracted increasing attention due to the increasing stringent regulations for environment protection and potential use in fuel cells in the future.[1,2] The sulfur compounds in fuels may have negative effects on the environment. Organic sulfur compounds can be transformed into SO_x when combusted in engines, which may react with water in the atmosphere to form acid rain, damaging buildings, leading to loss of forests and other problems.[3] Sulfur compounds can also poison some catalysts in exhaust gas converters for reducing CO and NO_x emissions, and cause corrosion problems in refining equipment.[4] The EPA in the United States has reduced the sulfur content in fuel to 30 ppm in gasoline and 15 ppm in diesel since 2006.[5]

Industrially, hydrodesulfurization is used to reduce the sulfur content in refineries. HDS is efficient to remove sulfur species with relative ease, such as thiols, sulfides and disulfides from oils, but less effective to remove thiophene, benzothiophene, dibenzothiophene and their derivatives, because of their aromatic characters.[6] In addition, the HDS technology is operated at temperatures in the range of 300–450 °C, and at H_2 pressure of 3.0–5.0 MPa, usually with $CoMo/Al_2O_3$ or $NiMo/Al_2O_3$ catalysts.[7,8] Under such conditions, olefins will react with H_2 to form alkanes, resulting to significant loss of octane number and excess consumption of H_2.[9] The lower reactivity of these aromatic sulfur compounds is much attributed to steric hindrance. It is reported that the removal of aromatic sulfur compounds by HDS process to the standard levels would require more than three-fold increase in the catalyst volume/reactor size, resulting in an enormously high cost of operation for higher temperature and higher pressure process.[10,11] Thus, it is imperative to develop non-HDS technologies to meet the need for fuels with low sulfur content, such as oxidative desulfurization,[12,13] biodesulfurization,[14,15] and adsorptive desulfurization.[16,17]

Compared to the hydrodesulfurization process, the adsorptive removal of sulfur compounds seems very promising from the point of energy consumption because the adsorption can be carried out at low temperature and pressure, and the sulfur content in the fuels can be reduced to a very low level.[18] So far, a various of materials used as adsorbents were studied for desulfurization such as active carbon,[19–21] metal oxides,[22,23] and zeolite-based materials.[24,25] Zeolites, especially FAU type adsorbent, have been investigated widely in desulfurization of transformation due to their high surface area and thermal and mechanical stabilities.

Except the experimental studies, a mathematical modeling is an efficient method for analysis of the chemical processes. There are different theoretical and empirical models used to fit the experimental data. It seems that using this method in understanding and simulating the adsorptive removal of sulfur compounds from fuels can reduce the cost of experiments and increases the feasibility of the process. Therefore, the study of adsorption process from both experimental and theoretical aspects is important. The theoretical models include the Langmuir and Freundlich models. There are several empirical models for modeling of adsorption kinetics, including the pseudo-first-order, pseudo-second-order and pseudo-*n*-order. The advantage of the empirical models is their simplicity.[26]

Tianjin Key Laboratory of Applied Catalysis and Technology, Department of Catalysis Science and Engineering, School of Chemical Engineering and Technology, Tianjin University, 300354, China. E-mail: xxy@tju.edu.cn; Fax: +86 2227401018; Tel: +86 2227401018

† The two authors contributed equally to this paper.

To the best of our knowledge, the use of NaY zeolites modified with $Ni(NO_3)_2$ and $Ce(NO_3)_3$ successively in the field of adsorption desulfurization has few reported. In Wang's work,[27] the influence of Ce loading, toluene, catalyst/oil ratio on the sulfur removal onto NiCeY were analyzed. The results indicated that NiCeY possessed higher sulfur adsorption quantity than NiY and CeY. In this study, NiCeY was prepared to investigated the adsorption kinetics, isotherm and thermodynamics on the removal of thiophene and benzothiophene. The parameters were calculated using different models.

2. Experiments

2.1 Materials

Zeolites NaY (power form, $SiO_2/Al_2O_3 = 2.5$) was obtained from Nankai Catalyst Technical Corporation. Thiophene (TP, 99%) and benzothiophene (BT, 99%) were bought from Tianjin Guangfu Fine Chemical Research Institute and Beijing Ouhe Technology respectively. *N*-Octane (AR) purchased from Tianjin Kuwait corporation was as solvent in experiment. All reagents were used without further purification.

2.2 Adsorbent preparation

Prior to the ion exchange, the zeolites NaY was dehydrated at a rate of 2 °C per minute to 300 °C by heating in muffle furnace and kept at 300 °C for 2 h. NiY zeolites was prepared by ion exchanging NaY with a 0.1 mol L^{-1} $Ni(NO_3)_2$ solution at 50 °C for 4 h. The ratio of the solution volume (mL) to the mass of zeolites (g) was 10 : 1. After ion exchange, the obtained NiY zeolites was filtered, washed thoroughly with distilled water to remove the residuary Ni^{2+}. The filtered cake was then dried at 110 °C for 5 h and calcined at 500 °C for 4 h. Both the obtained NiY and 0.1 mol L^{-1} $Ce(NO_3)_3$ aqueous solution were added to three-neck flask, and kept at 50 °C for 4 h. After filtering, washing, drying at 110 °C for 5 h, the zeolite was calcined at 500 °C for 4 h and we get the NiCeY zeolites. The color of the zeolites NiCeY changed from white to yellow after calcination, suggesting the oxidation of Ce^{3+} to Ce^{4+}.

The obtained NiCeY zeolite was grinded in the agate mortar sufficiently and shifted to glass desiccator immediately to avert the adsorption of water in air, reducing the adsorption capacity of thiophene and benzophene.

2.3 Preparation of model oil

Thiophene, benzothiophene and *n*-octane were used as the model components for compound containing sulfur and hydrocarbon in diesel desulfurization, respectively. Several model diesel fuels containing different concentration of sulfur were prepared and the detailed composition of the model fuels were listed in Table 1.

2.4 Adsorptive desulfurization

Prior to the adsorption experiment, the zeolites NiCeY was dried in oven at 110 °C for 2 h in order to remove the physically adsorbed water. The adsorption experiment was carried out using static method at a certain temperature and atmospheric pressure. The dried zeolites (0.40 g) was mixed with 28 mL model fuel in three-neck flask rapidly. After 1 h, the desulfurized fuel was stewed and sampled, and the sulfur content of model fuel before and after adsorption was analyzed by a FID-gas chromatograph (Agilent, GC-6820) equipped with a capillary column (FFAP, 60 m × 0.25 mm × 0.32 μm). The temperatures set in the injector, oven and detector were 250, 200, 250 °C, respectively.

Table 1 The compositions of model diesels

Ms	S content (mmol L^{-1})	Compositions
M1	21.92	Thiophene/*n*-octane
M2	17.54	Thiophene/*n*-octane
M3	13.15	Thiophene/*n*-octane
M4	8.77	Thiophene/*n*-octane
M5	4.38	Thiophene/*n*-octane
M6	21.92	Benzothiophene/*n*-octane
M7	17.54	Benzothiophene/*n*-octane
M8	13.15	Benzothiophene/*n*-octane
M9	8.77	Benzothiophene/*n*-octane
M10	4.38	Benzothiophene/*n*-octane

The adsorption capacity was calculated using the following equation:

$$q_t = \frac{(c_0 - c_t)V}{m} \quad (1)$$

The sulfur removal (*R*%) was calculated according to the formula:

$$R\ (\%) = \frac{c_0 - c_e}{c_0} \times 100\% \quad (2)$$

where V is the volume of the model fuel (mL), and m (g) is the mass of adsorbent; c_0, c_e and c_t (mmol L^{-1}) is the initial, equilibrium and t (min) concentration of sulfur in the model fuel, respectively.

3. Results and discussion

3.1 Effect of adsorption temperature

Generally, the effect of adsorption temperature on desulfurization experiment has two sides. Increasing the temperature would increase the diffusion rate of TP and BT in *n*-octane obviously, due to the decline of the viscosity in the solution. Meanwhile, too high temperature would enhance the desorption rate, thus reducing the adsorption capacity. Fig. 1 shows the effect of adsorption temperature on the adsorption capacity of TP and BT by using M1 and M6 as model fuel. It is observed that the adsorption capacity of thiophene and benzothiophene increased primarily from 0.65 to 0.70 mmol g^{-1} and 1.27 to 1.32 mmol g^{-1}, then dropped to 0.67 and 1.29 mmol g^{-1} respectively when the temperature rised to 90 °C. From the results in Fig. 1, it can be concluded that the suitable adsorption temperature is 70 °C.

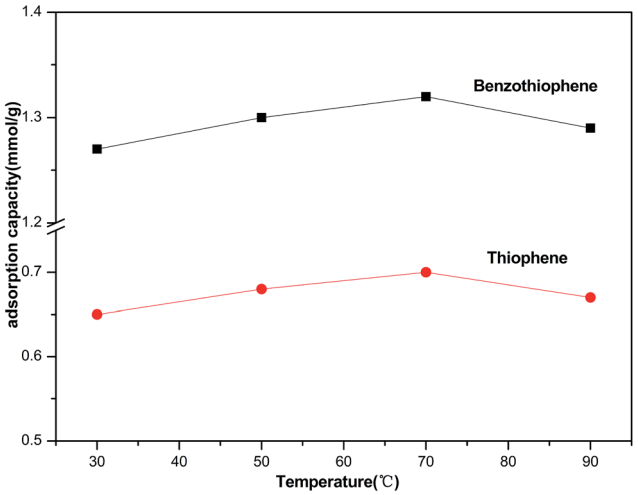

Fig. 1 Effect of temperature (30 °C, 50 °C, 70 °C, 90 °C) on the adsorption removal of thiophene and benzothiophene over NiCeY zeolites (model oil M1/M6: 7.00 mL; adsorbent: 0.10 g; contact time: 1 h).

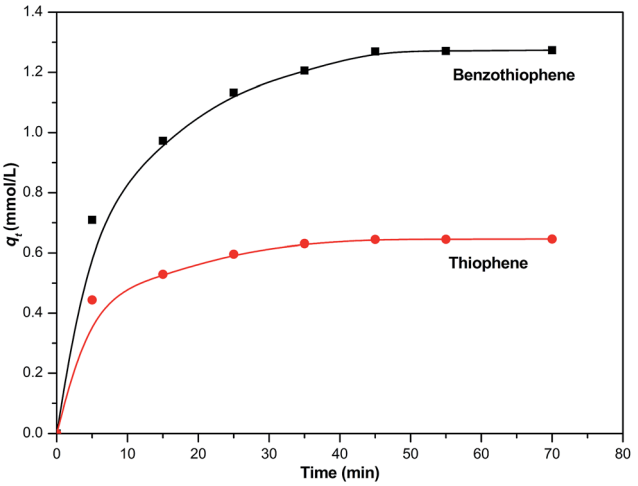

Fig. 2 Effect of adsorption time on the removal of thiophene and benzothiophene over NiCeY zeolites (model oil M1/M6: 28.00 mL; adsorbent: 0.40 g; temperature: 30 °C).

3.2 Effect of contact time on adsorption

The contact time to reach the equilibrium relied on the adsorption temperature and other variables. In the experiment, different contact time experiments were carried out on NiCeY at 30 °C using model fuel M1 and M6. The effect of contact time on the adsorption of TP and BT is shown in Fig. 2. The adsorption capacity of TP and BT over NiCeY increased rapidly and achieved over 70.28% and 70.56% in the first 5 min, then increased slowly as the time was prolonged. When the time was equal to 45 min, q_t became stable. It may have achieved equilibrium adsorption and the equilibrium adsorption capacity of TP and BT follows: BT > TP. Therefore, the equilibrium adsorption amount can be obtained in 45 min.

3.3 Effect of initial sulfur content on adsorption

The effect of the initial sulfur concentration on the adsorption of thiophene and benzothiophene at 30 °C is shown in Fig. 3. It is observed that the adsorptive capacity of thiophene and benzothiophene varied with its initial concentration. At the initial low sulfur content, the adsorption capacity of TP or BT increase rapidly and then increase gradually with increasing the sulfur content. This indicates that an increase in the initial concentration of sulfur leads to an increase in the adsorption capacity of TP and BT.

3.4 Equilibrium isothermal adsorption

In our study, the equilibrium isothermal adsorption was progressed by using model diesel (M1–M10, respectively) with a contact time of 1 h at 30, 50 and 70 °C. The plot of the equilibrium adsorptive capacity of sulfur per gram of NiCeY zeolites against the equilibrium concentration of sulfur in the fuel are shown in Fig. 4. As can be seen from Fig. 4, initially, q_e increases quickly with an increase of equilibrium concentration of sulfur, and then increases slightly. This indicates that most of the sulfur compounds could be adsorbed by NiCeY zeolites with the

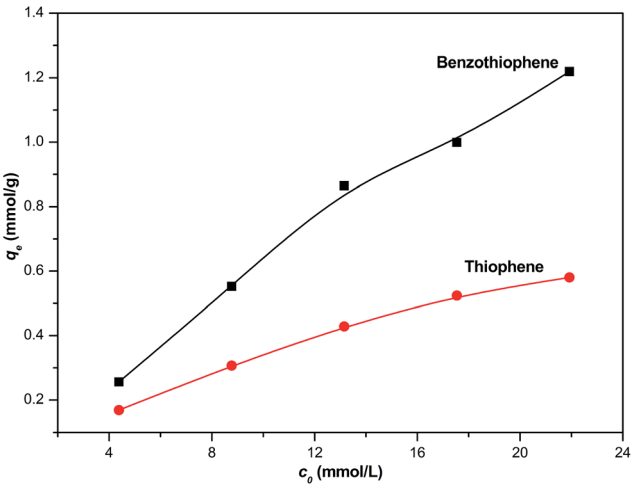

Fig. 3 Effect of initial sulfur content on the adsorption of thiophene and benzothiophene over NiCeY zeolites (model oil of M1–M10: 7.00 mL; adsorbent: 0.10 g; temperature: 30 °C).

initial concentration of sulfur lower. However, with an increase of sulfur concentration, the adsorption capacity of NiCeY zeolites may reach its saturation and the equilibrium adsorptive capacity (q_e) tends to be the maximum adsorption capacity (q_m) (Fig. 5).

The Langmuir model is possibly the most known and widely used sorption isotherm. It can fit to the experimental data. Generally, the interaction between the adsorbates and the adsorbent in solution includes two processes, namely, adsorption and desorption. The rates of adsorption (v_{ads}) and desorption (v_d) can be expressed as:

$$v_{ads} = k_{ads} c_t (1 - \theta) \quad (3)$$

$$v_d = k_d \theta \quad (4)$$

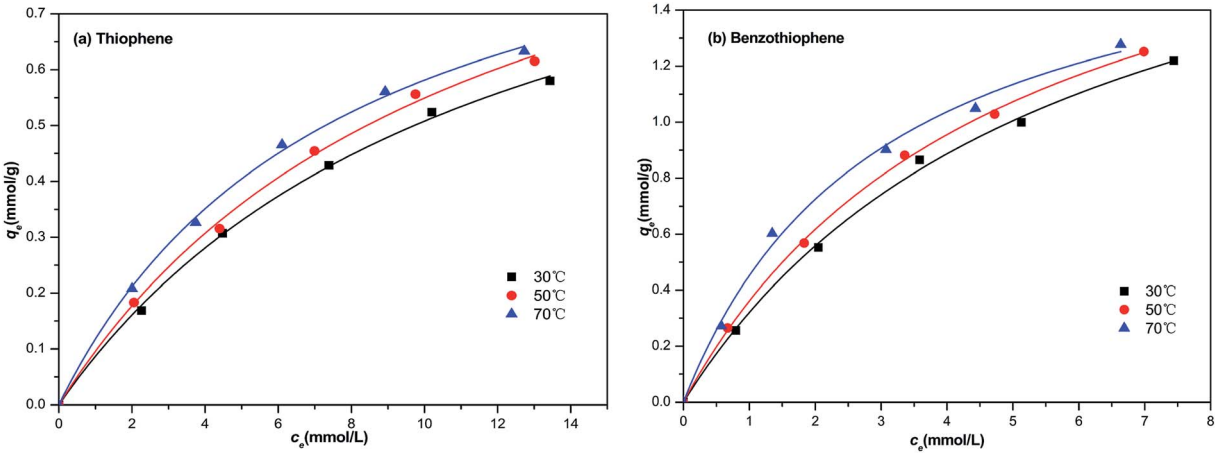

Fig. 4 Langmuir model equation used for the adsorption of (a) TP and (b) BT on NiCeY zeolites at different temperatures (30 °C, 50 °C, 70 °C).

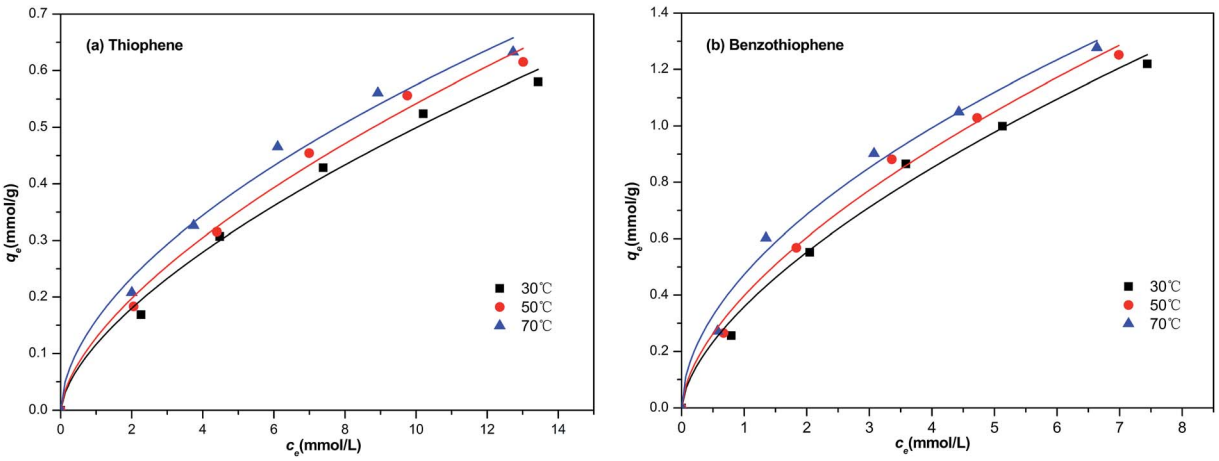

Fig. 5 Freundlich model equation used for the adsorption of (a) TP and (b) BT on NiCeY zeolites at different temperatures (30 °C, 50 °C, 70 °C).

where, k_{ads} and k_d are the adsorptive and desorptive constants, respectively; c_t is the content of sulfur in model diesel at time t; θ is the coverage ratio of the adsorbent surface, which can be calculated by q_t/q_m, whereby q_t and q_m represents the adsorption capacity at time t and the maximum adsorption amount. When the adsorption rate is equal to desorption rate, namely, $v_{ads} = v_d$. The concentration of sulfur (c_t) and the adsorption capacity (q_t) can be written as c_e and q_e. Therefore, the Langmuir isothermal model can be described as:[28]

$$q_e = \frac{K_L c_e q_m}{1 + K_L c_e} \quad (5)$$

where K_L represents the Langmuir constant, reflecting the affinity of binding sites. The values of K_L and q_m are calculated from the eqn (5).

The Freundich isotherm is expressed by an empirical model that suppose heterogeneous adsorption because of the diversity of adsorption sites and can be described as:[29]

$$q_e = K_F c_e^{1/n} \quad (6)$$

where K_F and n represent Freundlich constants indicative of adsorption capacity and adsorption intensity, respectively.

The calculated parameters and the correlation coefficient at different temperature are shown in Tables 2 and 3. From Table 2, we can find that with the increase of temperature, the Langmuir constant increase from 0.085 to 0.128 and from 0.175 to 0.330 for thiophene and benzothiophene adsorption on NiCeY zeolites. The obtained q_m increase from 1.03 to 1.16 and 1.82 to 2.15 mmol g^{-1} with temperature range from 30 to 70 °C, this means increasing temperature is beneficial for thiophene and benzothiophene adsorption. The correlation coefficient at 30 °C, 50 °C, 70 °C are all above 0.990, manifesting that the experimental data can be fitted with Langmuir model well, thiophene and benzothiophene are monolayer adsorption on NiCeY zeolites. From Table 3, with the increase of temperature, the obtained K_F increase from 0.116 to 0.158 and from 0.358 to 0.473, indicating the adsorption capacity increase with temperature. The obtained n is above 1.5, meaning adsorption process can occur easily.

Table 2 The calculated Langmuir adsorption isotherm parameters

	Parameters	30 °C	50 °C	70 °C
Thiophene	q_m (mmol g^{-1})	1.03	1.10	1.16
	K_L (L mmol^{-1})	0.085	0.090	0.128
	R^2	0.996	0.995	0.994
Benzothiophene	q_m (mmol g^{-1})	1.82	2.10	2.15
	K_L (L mmol^{-1})	0.175	0.206	0.330
	R^2	0.996	0.997	0.995

Table 3 The Freundlich adsorption isotherm parameters

	Parameters	30 °C	50 °C	70 °C
Thiophene	n	1.57	1.59	1.78
	K_F (L mmol^{-1})	0.116	0.128	0.158
	R^2	0.991	0.991	0.988
Benzothiophene	n	1.60	1.66	1.86
	K_F (L mmol^{-1})	0.358	0.398	0.473
	R^2	0.957	0.958	0.965

3.5 Kinetic study

3.5.1 Pseudo-first order, pseudo-second order models. The transport process of adsorbate from the solution into the pores on the adsorbent is a complicated process, containing external diffusion, pore diffusion, surface diffusion, and adsorption. NiCeY zeolites can adsorb the organic sulfur compounds mainly through two types of adsorption modes: π-complexation between Ni^{2+} ions and sulfur rings and direct coordination *via* S atoms with Ce^{4+} (S–M) interaction.[30,31] Thus, to better understand the adsorption desulfurization process, the kinetic models was applied to fit the experimental data. Therefore, the pseudo-first order model, pseudo-second model were used to analyze the adsorption kinetics of the process on NiCeY zeolites.

The pseudo-first order rate equation can be expressed as:[32]

$$\frac{dq_t}{dt} = k_1(q_e - q_t) \quad (7)$$

where q_t (mmol g^{-1}) is the adsorption capacity of sulfur on the NiCeY at time t (min), k_1 (min^{-1}) is the pseudo-first order rate constant and q_e (mmol g^{-1}) is the equilibrium adsorption capacity. After integration and applying the initial conditions, $t = 0$, $q_t = 0$. The eqn (8) can be written as:

$$q_t = q_e(1 - \exp(-k_1 t)) \quad (8)$$

The pseudo-second order rate equation is:[33]

$$\frac{dq_t}{dt} = k_2(q_e - q_t)^2 \quad (9)$$

where q_e is the equilibrium adsorption capacity (mmol g^{-1}), k_2 is the pseudo-second order rate constant (g mmol^{-1} min^{-1}). The integrated form of eqn (10) take the form:

$$q_t = \frac{k_2 q_e^2 t}{1 + k_2 q_e} \quad (10)$$

In this section, the two adsorption kinetic models such as pseudo-first-order model and pseudo-second-order model were used to fit the kinetic data of the TP and BT adsorption process on NiCeY. As can be seen in Fig. 6 and 7, the two adsorption kinetic models can fit to the experimental data well. In Tables 4 and 5, the calculated correlation coefficient R^2 of the pseudo-first-order model are less than the correlation coefficient R^2 of the pseudo-second-order model (>0.990), indicating that the pseudo-second-order model is slightly more favorable to fit the kinetics of the thiophene and benzothiophene adsorption (Fig. 8).

3.5.2 The effect of temperature on the adsorption kinetics. Generally, the temperature has two main effects on the adsorption process: (1) increasing the adsorption temperature will increase the rate of diffusion of the adsorbate in the solution due to the decrease of the velocity of the solution. (2) Changing the adsorption temperature of the process will lead to a new equilibrium adsorption capacity of the zeolites. Fig. 7 present the effect of temperature on the adsorption kinetics with model fuel M1 and M6.

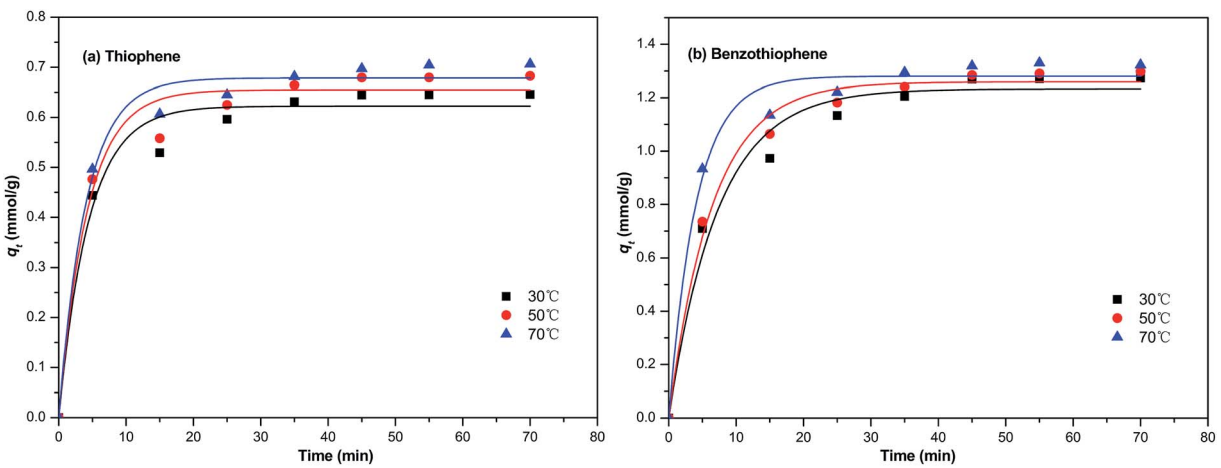

Fig. 6 The pseudo-first order model equation used for the adsorption of (a) TP and (b) BT on NiCeY zeolites at different temperatures (30 °C, 50 °C, 70 °C).

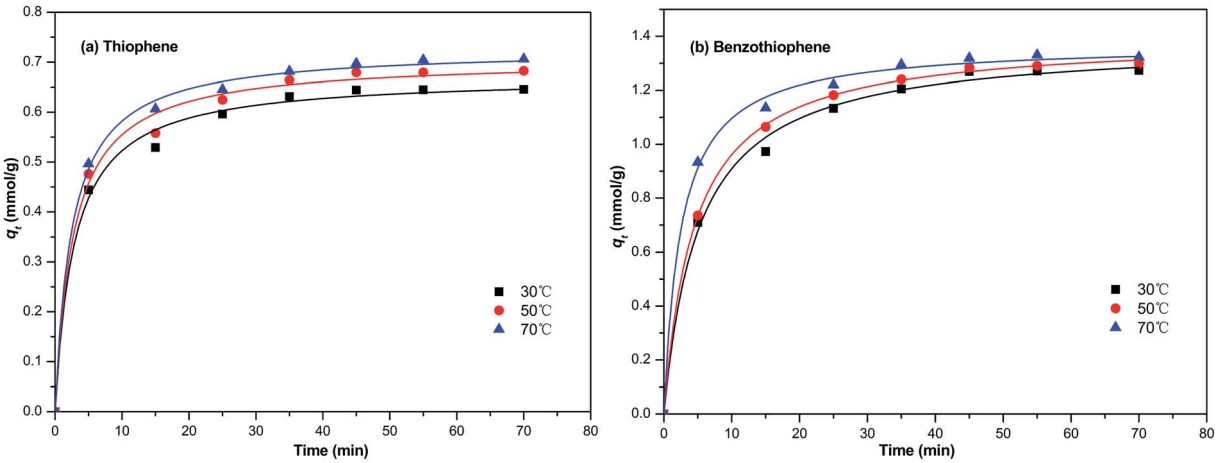

Fig. 7 The pseudo-second order model equation used for the adsorption of (a) TP and (b) BT on NiCeY zeolites at different temperatures (30 °C, 50 °C, 70 °C).

The experimental date was fitted with the non-linear pseudo-first order equation. The calculated parameters are shown in Table 5. It is seen that the equilibrium adsorption capacity and pseudo-second rate constant for the removal of TP and BT all increase with the increase of temperature. The date shows that the adsorption of TP and BT on NiCeY is much more effective at higher temperature.

The effect of adsorption temperature on the adsorption rate can be expressed with the Arrhenius equation:[34]

$$k_1 = k_0 \exp\left(\frac{-E_a}{R_g T_k}\right) \quad (11)$$

where k_0 (g mmol^{-1} min^{-1}) is the temperature independent factor; E_a (kJ mol^{-1}) is the activation energy of adsorption process; T_k is the absolute temperature in Kelvin; R_g (8.314 J mol^{-1} K^{-1}) is the universal gas constant, respectively. The equation can be written as:

$$\ln k_1 = \ln k_0 - \frac{E_a}{R_g T_k} \quad (12)$$

Generally, the slope of the plot of ln k_1 to $1/T$ is applied to calculate E_a based on the data shown in Table 4. Typically, the adsorption desulfurization process can be regarded as mass transfer control if the obtained activation energy is less than 21 kJ mol.[35] The activation energy 1.98 and 13.73 kJ mol^{-1} calculated lower than 21 kJ mol^{-1} for the adsorption of TP and BT on NiCeY zeolites indicate that the adsorption process is mass transfer controlled. The similar results can be found in ref. 36 and 37.

3.5.3 Diffusion study. The sorption of organic sulfur compounds on Y zeolites is a complex process. The adsorption can be controlled by the following steps: (1) the adsorbate diffuses from the diesel solution to the boundary layer of solution. (2) The adsorbate diffuses through the liquid film; (3) the pore diffusion and adsorption. One or two processes may be involved in the adsorption and the control of the adsorption is the slowest one.

A widely accepted kinetic model developed by Weber and Morris[38] shows that the sorption process may be diffusion controlled if the rate is dependent on the adsorbate and adsorbent diffusing towards one another. The intra-particle model is as:

$$q_t = k_i t^{0.5} + C \quad (13)$$

where k_i (mmol g^{-1} min$^{-0.5}$) is the intra-particle diffusion rate constant and C (mmol g^{-1}) is the constant related to the energy of adsorption. The intraparticle diffusion model constants can be calculated by the slope and intercept of the linear plot of q *versus* $t^{1/2}$, respectively.

The straight line of q_t to $t^{0.5}$ indicates the sorption process is diffusion controlled. However, if the data can be fitted with multiple lines, implying that more than one process is

Table 4 The pseudo-first order kinetic parameters obtained at 30, 50, 70 °C by the nonlinear fitting

	Parameters	30 °C	50 °C	70 °C
Thiophene	K_1 (min^{-1})	0.225	0.235	0.247
	q_e (mmol g^{-1})	0.62	0.65	0.68
	R^2	0.972	0.969	0.982
Benzothiophene	k_1 (min^{-1})	0.127	0.165	0.243
	q_e (mmol g^{-1})	1.23	1.25	1.28
	R^2	0.975	0.987	0.982

Table 5 The pseudo-second order kinetic parameters obtained at 30, 50, 70 °C by the nonlinear fitting

	Parameters	30 °C	50 °C	70 °C
Thiophene	k_2 (g mmol^{-1} min^{-1})	0.519	0.493	0.553
	q_e (mmol g^{-1})	0.67	0.72	0.73
	R^2	0.993	0.992	0.997
Benzothiophene	k_2 (g mmol^{-1} min^{-1})	0.140	0.158	0.282
	q_e (mmol g^{-1})	1.37	1.39	1.40
	R^2	0.996	0.999	0.997

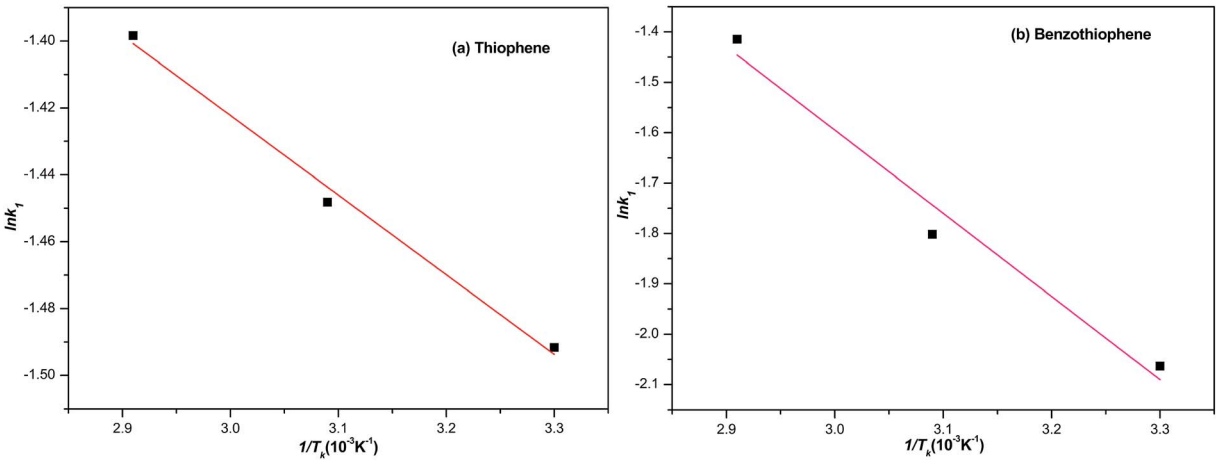

Fig. 8 The plot of ln k_1 to $1/T$.

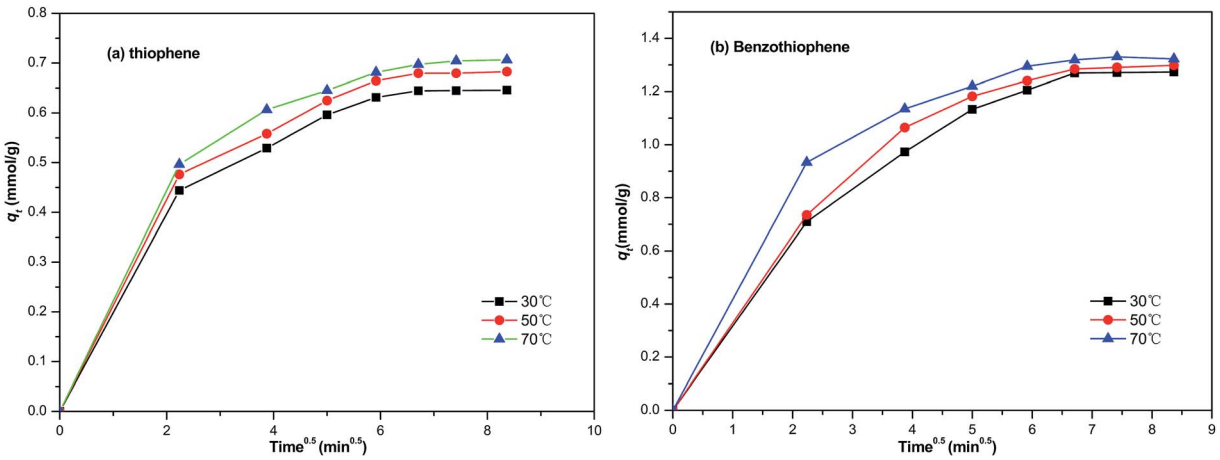

Fig. 9 The intra-particle diffusion model used for the adsorption of (a) TP and (b) BT on NiCeY zeolites.

controlling the adsorption process. As can be seen from Fig. 9, the plots are not linear, showing that adsorption is controlled by two processes. The initial portion indicates the boundary layer diffusion effect,[39] and the final linear portion is the result of intraparticle diffusion effect.[40]

Table 6 Thermodynamic parameters calculated for adsorption of TP and BT on NiCeY

	ΔH (kJ mol^{-1})	ΔS (J mol^{-1} K^{-1})	ΔG (kJ mol^{-1})		
			30 °C	50 °C	70 °C
Thiophene	−3.01	50.78	−8.60	−9.41	−10.13
Benzothiophene	−3.43	38.37	−11.96	−12.98	−14.00

3.6 Thermodynamic

The thermodynamic parameters such as free energy of sorption (ΔG), the heat of sorption and entropy changes (ΔH and ΔS) can be evaluated according to the following equations:[41]

$$K_d = q_e/c_e \quad (14)$$

where K_d is sorption distribution coefficient.

The K_d values are usually used to calculate the Gibbs free energy of sorption process at different temperatures.

$$\Delta G = -R_g T_k \ln K_d \quad (15)$$

where ΔG is the free energy of sorption (kJ mol^{-1}); T is the absolute temperature in Kelvin and R_g is the universal gas constant (8.314 J mol^{-1} K^{-1}).

The sorption distribution coefficient can be written as a function of temperature in the following:

$$\ln K_d = \frac{\Delta H}{R_g T_k} + \frac{\Delta S}{R} \quad (16)$$

where ΔH is the reaction heat of sorption process and ΔS is the enthalpy change of adsorption.

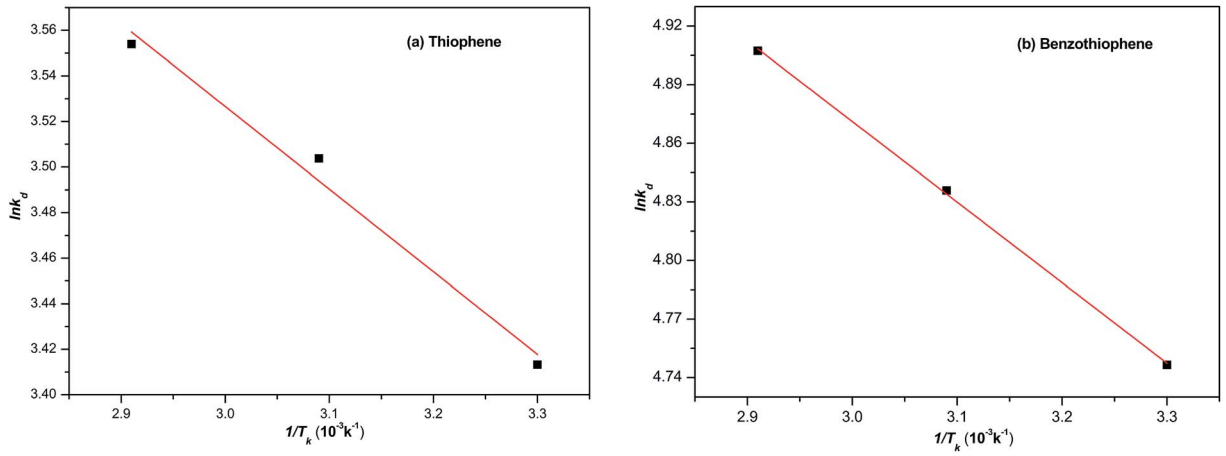

Fig. 10 The plot of ln k_d with $1/T_k$.

Table 7 Comparison of the adsorption capacity for different materials

Adsorbent	Adsorbate/solvent	C_0	Adsorption mode	q_e	Ref.
Activated carbon	BT/*n*-octane	300 ppm	Batch	1.29	42
Activated carbon	Real diesel	72 ppm	Fixed bed	0.05	43
NiY zeolites	Real diesel	297.2 ppm	Fixed bed	0.275	44
CeY zeolites	TP/*n*-heptane	3529 ppm	Fixed bed	1.15	45
MCM-41	FCC diesel	—	Fixed bed	—	46
SBA-15	DBT/diesel	564 ppm	Batch	0.31	47
NiCeY	TP/BT/*n*-octane	1000 ppm	Batch	0.64/1.27	This work

The thermodynamic parameters such as the heat of sorption (ΔH), free energy of sorption (ΔG) and enthalpy change of adsorption (ΔS) were calculated using eqn (4)–(6). The temperature used was ranging from 30 to 70 °C. The Gibbs free energy (ΔG) means the degree of spontaneity of the sorption process and the higher negative value reflects a more energetically favourable sorption. ΔH and ΔS were obtained from the intercept and slop of a plot of ln K_d against $1/T_k$ (Fig. 10). The calculated parameters are listed in Table 6. The negative value of Gibbs free energy change ($\Delta G < 0$) indicates that the adsorption of either TP or BT on NiCeY zeolites is a spontaneous process. The value of ΔG becomes more negative with temperature increase. This indicates that the adsorption process is favoured with the increase of temperature. The negative value of ΔH manifest that the adsorption of TP or BT was exothermic and the positive value of ΔS shows the increase of freedom at liquid/solid interface during the adsorption process.

3.7 Investigation of adsorption capacity comparison and regeneration

Due to the difficulty in comparing the sulfur adsorption performance using zeolites here with previous ones, the adsorption comparison may be favorable for the future works. The materials used as adsorbents previously reported, together with the experimental conditions and adsorption capacity are compared in Table 7. As shown in Table 7, We list the comparisons including the adsorption of thiophene, benzothiophene and dibenzothiophene compounds because much work has been done in adsorption desulfurization area.

Finally, regeneration of the NiCeY zeolites was investigated, the common applied regeneration methods were thermal treatment and solvent extraction. In our work, we applied both

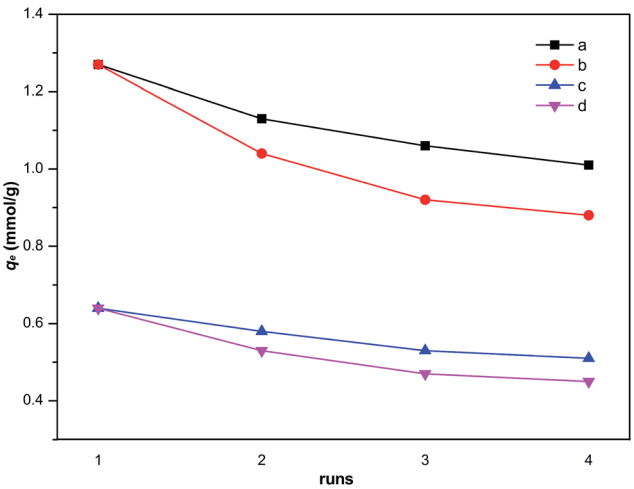

Fig. 11 Regeneration adsorption of thiophene and benzothiophene for NiCeY zeolites by thermal treatment and solvent extraction (initial sulfur concentration: 1000 ppm; T = 30 °C; (a) benzothiophene, solvent extraction; (b) benzothiophene, thermal treatment; (c) thiophene, solvent extraction; (d) thiophene, thermal treatment).

methods to investigate the adsorption performance of NiCeY zeolites. After the first adsorption, the zeolites was separated by centrifugation, dried at 200 °C overnight and then calcinated at 500 °C for 4 h in air atmosphere for the next adsorption run. We also investigated a solvent extraction method for regenerating the adsorbent. The zeolites used was separated by centrifugation, washed with ethanol at room temperature, and then dried for the next adsorption run.

As shown in Fig. 11, the zeolites regenerated by solvent extraction has higher adsorption capacity compared with thermal treatment regeneration method. And the sulfur adsorption capacity declined slightly after the fourth run, indicating the satisfactory reusability of the NiCeY zeolite.

4. Conclusions

In this work, the NiCeY zeolites was prepared and used to adsorb sulfur compounds in diesel. The experimental results showed that NiCeY zeolites could effectively remove thiophene and benzothiophene, and the adsorption capacity for TP and BT reach 0.70 and 1.32 mmol g^{-1}, respectively. The equilibrium adsorption on NiCeY zeolites was achieved for 60 min and the adsorption capacity of TP or BT increased with an increase of initial sulfur content and adsorption temperature. The equilibrium isotherms indicate that the adsorption can be described by the Langmuir model better than the Freundlich model. The kinetics analysis show that the adsorption processes can be fitted suitably by the pseudo-second order model with higher R^2. The calculated activation energies for the adsorption of TP and BT on NiCeY zeolites are 1.98 and 13.73 kJ mol^{-1}, suggesting the adsorption is mass transfer controlled. Besides, the Diffusion study indicates that the adsorption of TP and BT on NiCeY zeolites was controlled by two steps. The analysis of the thermodynamics indicate that the adsorption of TP and BT are spontaneous and exothermic.

References

1 J. H. Shan, L. Chen, L. B. Sun, *et al.*, *Energy Fuels*, 2011, **25**(7), 3093–3099.
2 C. Song, *Catal. Today*, 2003, **86**(1), 211–263.
3 J. Xiao, X. Wang, M. Fujii, *et al.*, *AIChE J.*, 2013, **59**(5), 1441–1445.
4 L. Wu, J. Xiao, Y. Wu, *et al.*, *Langmuir*, 2014, **30**(4), 1080–1088.
5 EPA, US Environmental Protection Agency, April 2003, http://www.epa.gov/nonroad/f03008.htm#q3.
6 H. Tang, Q. Li, Z. Song, *et al.*, *Catal. Commun.*, 2011, **12**(12), 1079–1083.
7 Y. Sun and R. Prins, *Angew. Chem., Int. Ed.*, 2008, **47**(44), 8478–8481.
8 F. Tian, X. Yang, Y. Shi, *et al.*, *J. Nat. Gas Chem.*, 2012, **21**(6), 647–652.
9 V. C. Srivastava, *RSC Adv.*, 2012, **2**(3), 759–783.
10 C. Song and X. Ma, *Appl. Catal., B*, 2003, **41**(1), 207–238.
11 M. Breysse, G. Djega-Mariadassou, S. Pessayre, *et al.*, *Catal. Today*, 2003, **84**(3), 129–138.
12 W. Zhu, J. Zhang, H. Li, *et al.*, *RSC Adv.*, 2012, **2**(2), 658–664.
13 A. D. Bokare and W. Choi, *J. Hazard. Mater.*, 2016, **304**, 313–319.
14 G. Mohebali and A. S. Ball, *Int. Biodeterior. Biodegrad.*, 2016, **110**, 163–180.
15 A. Pathak, D. J. Kim and B. G. Kim, *International Journal of Environmental, Chemical, Ecological, Geological and Geophysical Engineering*, World Academy of Science, Engineering and Technology, 2016, vol. 8(8), pp. 618–621.
16 X. Ma, L. Sun and C. Song, *Catal. Today*, 2002, **77**(1), 107–116.
17 A. J. Hernández-Maldonado and R. T. Yang, *J. Am. Chem. Soc.*, 2004, **126**(4), 992–993.
18 M. Muzic, K. Sertic-Bionda and Z. Gomzi, *Chem. Eng. Technol.*, 2008, **31**(3), 355–364.
19 M. T. Timko, J. A. Wang, J. Burgess, *et al.*, *Fuel*, 2016, **163**, 223–231.
20 G. I. Danmaliki and T. A. Saleh, *J. Cleaner Prod.*, 2016, **117**, 50–55.
21 V. Selvavathi, V. Chidambaram, A. Meenakshisundaram, *et al.*, *Catal. Today*, 2009, **141**(1), 99–102.
22 S. Velu, X. Ma, C. Song, *et al.*, *Energy Fuels*, 2005, **19**(3), 1116–1125.
23 Y. Wang, R. T. Yang and J. M. Heinzel, *Ind. Eng. Chem. Res.*, 2008, **48**(1), 142–147.
24 A. Shams, A. M. Dehkordi and I. Goodarznia, *Energy Fuels*, 2007, **22**(1), 570–575.
25 Y. Shi, W. Zhang, H. Zhang, *et al.*, *Fuel Process. Technol.*, 2013, **110**, 24–32.
26 H. Song, Y. Chang, X. Wan, *et al.*, *Ind. Eng. Chem. Res.*, 2014, **53**(14), 5701–5708.
27 J. Wang, F. Xu, W. Xie, *et al.*, *J. Hazard. Mater.*, 2009, **163**(2), 538–543.
28 I. Langmuir, *J. Am. Chem. Soc.*, 1917, **3**(9), 1848–1906.
29 H. M. F. Freundlich, *J. Phys. Chem.*, 1906, **57**, 385–471.
30 A. J. Hernández-Maldonado, F. H. Yang, G. Qi, *et al.*, *Appl. Catal., B*, 2005, **56**(1), 111–126.
31 H. Wang, L. Song, H. Jiang, *et al.*, *Fuel Process. Technol.*, 2009, **90**(6), 835–838.
32 S. Lagergren, PA Norstedt & soner, 1898, **24**(4), 1–39.
33 Y. S. Ho and G. McKay, *Process Biochem.*, 1999, **34**(5), 451–465.
34 K. J. Laidler, *J. Chem. Educ.*, 1984, **61**(6), 494.
35 R. Haque, F. T. Lindstrom, V. H. Freed, *et al.*, *Environ. Sci. Technol.*, 1968, **2**(3), 207–211.
36 J. Jiang and F. T. T. Ng, *Adsorption*, 2010, **16**(6), 549–558.
37 K. Banerjee, P. N. Cheremisinoff and S. L. Cheng, *Water Res.*, 1997, **31**(2), 249–261.
38 W. J. Weber and J. C. Morris, *Journal of the Sanitary Engineering Division*, 1963, **89**(2), 31–60.
39 M. Montazerolghaem, A. Rahimi and F. Seyedeyn-Azad, *Appl. Surf. Sci.*, 2010, **257**(2), 603–609.
40 D. Reichenberg, *J. Am. Chem. Soc.*, 1953, **75**(3), 589–597.
41 N. Bektaş, B. A. Agım and S. Kara, *J. Hazard. Mater.*, 2004, **112**(1), 115–122.
42 Y. Shi, X. Zhang and G. Liu, *ACS Sustainable Chem. Eng.*, 2015, **3**(9), 2237–2246.

43 C. Mariin-Rosas, L. F. Ramiírez-Verduzco, F. R. Murrieta-Guevara, *et al.*, *Ind. Eng. Chem. Res.*, 2010, **49**(9), 4372–4376.
44 A. J. Hernandez-Maldonado and R. T. Yang, *Ind. Eng. Chem. Res.*, 2004, **43**(4), 1081–1089.
45 L. Lin, Y. Zhang, H. Zhang, *et al.*, *J. Colloid Interface Sci.*, 2011, **360**(2), 753–759.
46 B. S. Liu, D. F. Xu, J. X. Chu, *et al.*, *Energy & fuels*, 2007, **21**(1), 250–255.
47 Y. Shi, G. Liu and X. Zhang, *Ind. Eng. Chem. Res.*, 2017, **56**, 2557–2564.